Quench front progression in a superheated porous medium: experimental analysis and model development

Andrea Bachrata, Florian Fichot, Georges Repetto, Michel Quintard, Joëlle Fleurot

Quench Front Progression in a Superheated Porous Medium: Experimental Analysis and Model Development

Andrea Bachrata[1], Florian Fichot[1], Georges Repetto[1], Michel Quintard[2, 3] and Joelle Fleurot[1]

1. Institut de Radioprotection et de Sûreté Nucléaire, Cadarache 13115, France

2. IMFT (Institut de Mécanique des Fluides de Toulouse), Université de Toulouse, Toulouse F-31400, France

3. CNRS (Centre National de la Recherche Scientifique), IMFT, Toulouse F-31400, France

Abstract: In case of accident at a nuclear power plant, water sources may not be available for a long period of time and the core heats up due to the residual power. Any attempt to inject water during core degradation can lead to quenching and further fragmentation of core material. The fragmentation of fuel rods and melting of reactor core materials may result in the formation of a "debris bed". The typical particle size in a debris bed might reach few millimeters (characteristic length-scale: 1-5 mm). The two-phase flow model for reflood of the degraded core is briefly introduced in this paper. It is implemented into the ICARE-CATHARE code, developed by IRSN (Institut de radioprotection et de sûreté nucléaire), to study severe accident scenarios in pressurized water reactors. Currently, the French IRSN sets up two experimental facilities to study debris bed reflooding, PEARL and PRELUDE, and validate safety models. The PRELUDE program studies the complex two phase flow (water/steam), in a porous medium (diameter 180 mm, height 200 mm), initially heated to a high temperature (400 °C or 700 °C). On the basis of the experimental results, thermal hydraulic features at the quench front have been analyzed. The two-phase flow model shows a good agreement with PRELUDE experimental results.

Key words: Severe accident, reflood, debris bed, two-phase flow model.

1. Introduction

In case of severe accident in a nuclear reactor, water sources are not available for a long period of time and the reactor core heats up due to the residual power. This leads to cladding oxidation and, possibly, to the collapse of fuel rods and melting of reactor core materials that can result in the formation of a "debris bed". In a debris bed, the particles size would be a few millimeters (characteristic length-scale: 1-5 mm). If the core can not be cooled down, core melting and melt relocation to the lower plenum occurs. If the lower plenum is dry, the hot materials in contact with the vessel might endanger the integrity of the reactor pressure vessel wall. The aim of the severe accident management is to prevent the development of the above-mentioned scenario to more serious conditions. From a safety point of view, it is important to evaluate chances of coolability of the reactor core during a severe accident. This is in line with the safety philosophy of defence in depth which requires to foresee and to analyse all options to stop an accident at any stage.

Reflooding (injection of water) is possible if one or several water sources become available during the accident. An efficient use of those water sources may significantly contribute to the extension of safety margin of pressurized water reactors. If water source is available during the late phase of accident, water will enter a configuration of the reactor core that is largely modified and will resemble to the debris bed observed in TMI-2. The higher temperatures and smaller hydraulic diameters in a debris bed make the coolability more difficult than for intact fuel rods under

Corresponding author: Andrea Bachrata, Ph.D., research fields: thermohydraulics, severe accidents. E-mail: andrea.bachratakubic@cea.fr.

LOCA (loss of coolant accident) conditions. However, the successful reflood of such a severely damaged reactor core already happened during the TMI-2 accident [1]. On the other hand, it must also be recognized that at elevated core temperatures, the rate of oxidation of metals may be very high if steam is available. Therefore, reflood is likely to lead to an enhanced hydrogen formation and the risk of containment damage. The prediction of the core evolution in case of reflood requires an accurate modelling of both the heat transfer and the oxidation of metal (possibly molten). Thus, the reflood scenario of a severely damaged reactor core represents actually one of the major objectives of severe accident research. The present paper will only deal with the heat transfer issue.

2. Experimental Data

The available knowledge about core reflooding consists in international experimental programs that were performed in the past 30 years. Concerning debris beds, an important body of the experiments was initially focused on the determination of the critical heat flux, i.e., the maximum volumetric power that can be removed from a debris bed by water, e.g., the recent experiments STYX [2], SILFIDE [3]. Secondly, a series of dry-out experiments and also quenching experiments were performed at facilities POMECO [4] or DEBRIS [5]. The bottom and top reflooding experiments were studied by Ginsberg [6] or Tutu [7]. These two experimental programs brought interesting data for reflood analysis of debris bed initially at high temperature. These experimental results were used for validation of models implemented into European computer codes, WABE [8], ICARE-CATHARE [9], or American codes, MARCH, CONTAIN [6]. The actual experimental objectives are to ensure a more representative geometry and volumetric heating of the particles, compared to previous experiments. In addition, the actual measuring techniques could significantly enhance the database of experimental results. However, experimental techniques to measure local void fractions or velocities are still missing.

Currently, the French IRSN (Institut de Radioprotection et de Sûreté Nucléaire) sets up two experimental facilities, PRELUDE and PEARL (planned in 2012) to enhance the database of tests results. The main objectives are to extend the range of thermal-hydraulic conditions to higher temperatures and higher pressures than in previous tests [6, 7]. The objective is also to study 2D/3D effects during quenching. The PRELUDE experiment [10] is a preliminary test section, with smaller dimensions and running only at atmospheric pressure. That facility is used to optimize the induction heating and the measurement devices that should be used in PEARL facility. The PRELUDE geometry in Fig. 1 consists of a cylinder with an internal diameter of 174 mm filled with spherical steel particles of 4 mm, 2 mm or 1 mm. The height of the debris bed is fixed to 200 mm and the porosity is 0.4 mm. The debris bed is brought to its initial temperature by inductive heating that is maintained during reflood. The initial temperature is 400 °C, 700 °C or 1,000 °C. The outlet pressure is 1 bar. Liquid water is injected at 20 °C at the bottom of the debris bed. Four inlet superficial velocities were used, namely 0.555 mm/s, 1.38 mm/s, 2.77 mm/s and 5.55 mm/s.

The particle and fluid temperatures are measured at different positions. The steam flow is measured at the inlet and the outlet of the section and the difference of pressure across the particle bed is also measured. Reproducibility tests have been performed and have shown that outstanding disturbances observed in some measurements are not produced randomly but are reproduced for every test. Therefore, those disturbances result only from local non-homogeneities of the debris bed. The analysis presented in this paper concerns the PRELUDE tests with initial temperature 400 °C. The authors assume that the largest steam production occurs in the areas where the temperature is well below 400 °C, so a particular attention to modelling of heat transfer in that zone was done.

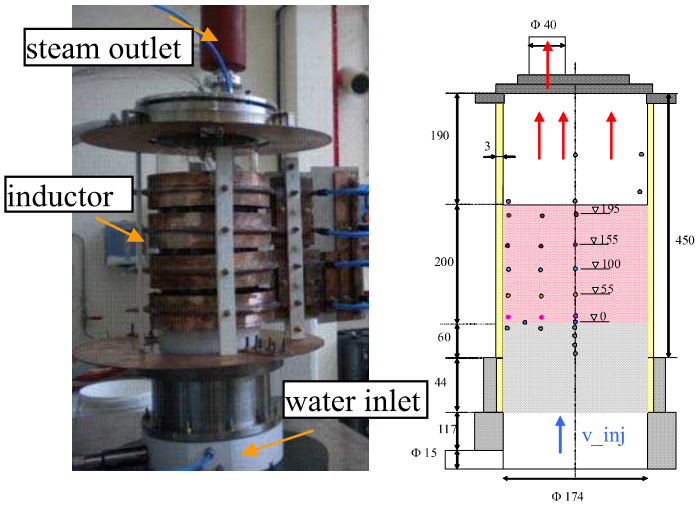

Fig. 1 PRELUDE experimental facility (in mm).

2.1 Analysis of Experimental Results

The velocity of the quench front is one of the key parameters to be validated in reflood analysis. First, the conditions of existence of a steady-state progression have to be analysed. It is interesting to study if a steady-state progression occurs because this will significantly help in future analysis of large scale and simplification of model. Moreover, when the steady-state progression exists, its velocity may be used to correlate some relevant parameters characterizing the particle bed or the water injection. The basic phenomenology that is summarized in this section comes from the interpretation of PRELUDE bottom-reflood experimental results. First, water enters the porous media that is initially at high temperature (e.g., 300-600 °C above the quenching temperature). The initial heat transfer and evaporation rate are low because the heat transfer coefficient is low due to film boiling. As water continues to progress, the first quenching of particles occurs at the bottom and thus, high evaporation rate occurs. From there, the quenching front starts to progress, initially with a velocity that is close to water injection velocity and, later, at a lower constant velocity (for most of the tests). The analysis of experimental data never showed a quench front velocity that was larger than the water injection velocity. The peak of steam production if it occurs (Fig. 2) will result

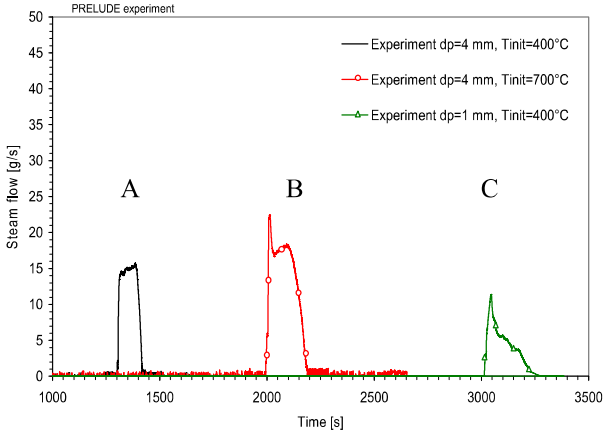

Fig. 2 Examples of steam flow production during reflood at different PRELUDE tests.

from that maximum initial quench front velocity and from the accumulation of water in the porous column. The similar behavior in a steam flow production was already observed in previous studies [7], but the measurements were not so accurate. When the progression becomes stable, the position of the quench front corresponds roughly to a balance between the cumulated evaporation rate downstream of the quench front position and the local water flow rate.

2.2 Steady State Progression of Quench Front

The quench front velocity is identified from the determination of the elevation where temperature is below the saturation temperature. It may be evaluated within the column for three different radii and five

different elevations (Fig. 1). It should be noted that the accuracy on the instant of quenching depends on the reference temperature that is taken for comparison. In Fig. 3, it can be seen that the saturation temperature is not a good reference because it is measured with some error (few degrees) and is not always stable. In order to be more accurate, it is better to take $T_{sat}+5$ or $T_{sat}-5$ as a reference temperature but the optimal value is not decided. Analyzing the PRELUDE experimental results, it can be concluded that there exists a steady state propagation of the quench front for all the cases considered here (Section 4.1). It indicates that the dynamic processes occurring in the bed are "fast" with respect to the injection velocity (no significant delay of quenching) but "stable" (no acceleration or dramatic increase of steam production). The quench front velocity is the same for the central and mid-radius positions. It is faster near the wall, probably because the initial temperature is lower and the porosity slightly higher. In the next section, it will be seen that the steady state propagation of the quench front allows a simpler analysis of model and experimental measurements.

2.3 Conversion Factor between Produced Steam and Injected Water

If there is a steady state propagation of the quench front, some balance equations may be simplified and some variables can be expressed as a function of the propagation velocity. The conversion factor between the produced steam flow and the injection liquid flow (Q_g/Q_l) is of particular interest. Adapting the formulations of Tutu et al. [7] and Tung and Dhir [11], the energy balance is written as:

$$\frac{Q_g}{Q_l} = \frac{\left[\begin{array}{l} v_{QF}(1-\varepsilon)\rho_s Cp_s(T_s - T_{sat}) \\ +v_l(1-\varepsilon)\rho_s Cp_s(T_{sat} - T_l) - v_l\rho_l\varepsilon Cp_l(T_{sat} - T_l) \end{array}\right]}{\left[\Delta h^{vap} + Cp_g(T_s - T_{sat})\right] v_l\rho_l\varepsilon} \quad (1)$$

where v_{QF} is the velocity of progression of quench front and T_s is the initial temperature of solid. From Fig. 4, it can be seen that there exists a simple relation between the quench front velocity and the conversion factor. In Fig. 4, it is clear that the measured quench front velocity is always lower than the liquid injection velocity. In Fig. 5, the experimental and calculated conversion factors are compared. The experimental conversion factors are presented only for test cases where a steady-state steam production was identified e.g., cases A and B in Fig. 2. It can be seen that the

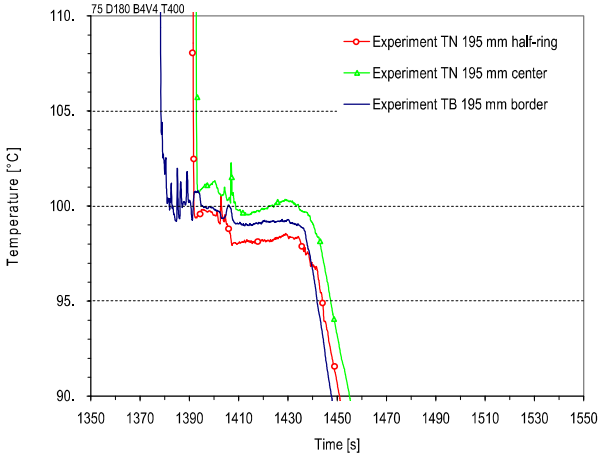

Fig. 3 Example of experimental measurements of temperature in pores.

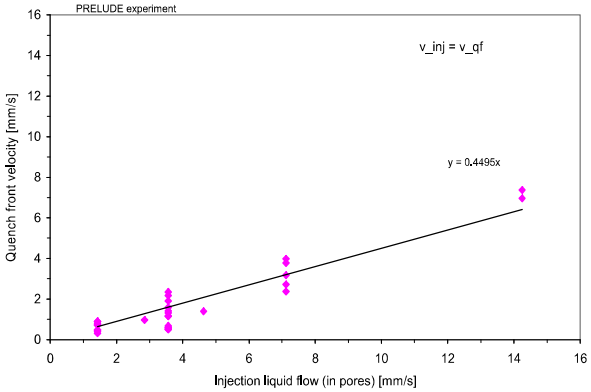

Fig. 4 Dependence of quench front velocity on injection liquid flow.

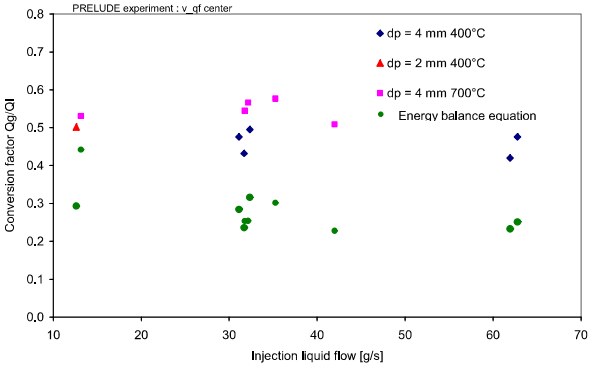

Fig. 5 Conversion factor between injected water and produced steam for different tests.

experimental conversion factors are higher than calculated. This may be due to the fact that the quench front velocity identified in the centre was taken to calculation but for most of the cases the quench front velocity at border was higher so the conversion factor is expected to be higher.

3. Modelling of Reflood Process

In this section, experimental results are used to validate a reflood model. Such a model for the three-dimensional two-phase flow in a heat-generating porous medium was earlier developed and assessed [12-14]. This model is recalled here, with some improvements.

3.1 Momentum Balance Equations

The friction forces between the solid matrix and the fluid phases are taken into account by using the classical extension of Darcy's law to two-phase flows. This means that viscous and inertial drag forces are calculated with relative permeabilities and passabilities coefficients, depending mainly on the void fraction using standard Brooks and Corey relation [15]. There is no explicit interfacial drag force between the liquid and gas phases. This may be missing in the model, as it was suggested by Schulenberg et al. [16], but there does not appear to be a satisfactory correlation available in the literature. Therefore, the momentum balance equations have a rather classical form, as follows:

$$\alpha\left\langle\rho_g\right\rangle^g\left(\frac{\partial\left\langle v_g\right\rangle^g}{\partial t}+\left\langle v_g\right\rangle^g.\nabla\left\langle v_g\right\rangle^g\right)=-\alpha\nabla\left\langle p_g\right\rangle^g \tag{2}$$
$$+\alpha\left\langle\rho_g\right\rangle^g g-\varepsilon\alpha^2\left(\frac{\mu_g}{Kk_{rg}}\left\langle v_g\right\rangle^g+\varepsilon\alpha\frac{\left\langle\rho_g\right\rangle^g}{\eta\eta_{rg}}\left\langle v_g\right\rangle^g\left|\left\langle v_g\right\rangle^g\right|\right)$$

$$(1-\alpha)\left\langle\rho_l\right\rangle^l\left(\frac{\partial\left\langle v_l\right\rangle^l}{\partial t}+\left\langle v_l\right\rangle^l.\nabla\left\langle v_l\right\rangle^l\right)=-(1-\alpha)\nabla\left\langle p_l\right\rangle^l \tag{3}$$
$$+(1-\alpha)\left\langle\rho_l\right\rangle^l g-\varepsilon(1-\alpha)^2\left(\frac{\mu_l}{Kk_{rl}}\left\langle v_l\right\rangle^l+\varepsilon(1-\alpha)\frac{\left\langle\rho_l\right\rangle^l}{\eta\eta_{rl}}\left\langle v_l\right\rangle^l\left|\left\langle v_l\right\rangle^l\right|\right)$$

In these equations, $\left\langle p_\beta\right\rangle^\beta$, $\left\langle\rho_\beta\right\rangle^\beta$, μ_β and $\left\langle v_\beta\right\rangle^\beta$ are respectively the intrinsic average pressure, density, dynamic viscosity and velocity of the β-phase ($\beta = g, l$). For uniform spherical particles, the intrinsic permeability and passability are correlated with the particle diameter d_p and the porosity ε by the Carman-Kozeny relation [17], and Ergun law [18]. The capillary pressure is introduced in the equations to represent macroscopically the effect of the pressure jump across the non-wetting/wetting phase interface.

3.2 Energy Balance Equations

Macroscopic energy conservation equations for the three phases are obtained by averaging the local energy conservation equations [19, 20]. The complete set of closure problems is presented in Ref. [19]. The averaged equations are simplified following [21] and the resulting macroscopic energy conservation equations are expressed as follows:

- gas phase

$$\frac{\partial\left(\alpha\varepsilon\left\langle\rho_g\right\rangle^g\left\langle h_g\right\rangle^g\right)}{\partial t}+\nabla.\left(\alpha\varepsilon\left\langle\rho_g\right\rangle^g\left\langle v_g\right\rangle^g\left\langle h_g\right\rangle^g\right)= \tag{4}$$
$$\nabla.\left(K_g^*\nabla.\left\langle T_g\right\rangle^g\right)+\dot{m}_g h_g^{sat}+Q_{pg}+Q_{gi}$$

- liquid phase

$$\frac{\partial\left((1-\alpha)\varepsilon\left\langle\rho_l\right\rangle^l\left\langle h_l\right\rangle^l\right)}{\partial t}+\nabla.\left((1-\alpha)\varepsilon\left\langle\rho_l\right\rangle^l\left\langle v_l\right\rangle^l\left\langle h_l\right\rangle^l\right)= \tag{5}$$
$$\nabla.\left(K_l^*\nabla.\left\langle T_l\right\rangle^l\right)+\dot{m}_l h_l^{sat}+Q_{pl}+Q_{li}$$

- solid phase

$$\frac{\partial\left((1-\varepsilon)\left\langle\rho_s\right\rangle^s\left\langle h_s\right\rangle^s\right)}{\partial t}= \tag{6}$$
$$\nabla.\left(K_s^*\nabla.\left\langle T_s\right\rangle^s\right)-Q_{pl}-Q_{pg}-Q_{pi}+\omega_s$$

In these equations, $\left\langle h_\beta\right\rangle^\beta$ and $\left\langle T_\beta\right\rangle^\beta$ are the macroscopic enthalpy and the temperature of the β-phase, respectively ($\beta = g, l, s$ for the gas, liquid and the solid phases). K_β^* is the effective thermal diffusion tensor including dispersion. The thermal exchanges between fluid phase and solid phase ($Q_{p\beta}$), fluid phase and interface ($Q_{\beta i}$) and solid phase and interface (Q_{pi}) are expressed as a heat transfer coefficient multiplied by the temperature difference.

3.3 Improvement of Heat Transfer Model

The porous medium temperature at the time of water injection may be significantly higher than the rewetting

temperature and complicated flow and heat transfer patterns are generated. At high surface temperatures corresponding to film boiling (Fig. 6), the cooling rate is rather low as the liquid is separated from the surface by a continuous vapor film. As temperature decreases below the minimum heat flux temperature (usually called Leidenfrost), a transition boiling regime is encountered, where an intermittent wetting of the surface occurs and the heat transfer rate increases with decreasing surface temperature. At a surface temperature corresponding to critical heat flux, the entire surface becomes available for wetting and intense nucleate boiling ensues, causing the surface to cool rapidly until the saturation temperature is reached, below which the surface is cooled by single-phase liquid convection. In our model, specific heat transfer coefficients were obtained analytically in simplified geometrical configurations as the stratified cell and Chang's cell [19]. For a stratified unit cell, two typical phase repartitions were considered, namely the solid-liquid-gas and the solid-gas-liquid repartition. The first refers to liquid being the wetting phase, the second refers to vapor being the "wetting" phase. As for the flow through the porous medium, the authors assume that the flow structure can correspond to a distribution in channels [22]. It is assumed that, for an oriented liquid flow in porous media, people can expect a phase repartition where one phase will be "wetting" and the second phase will eventually flow in the remaining pores under the form of bubbles or slugs. Because of this assumption, the effective properties obtained for a stratified unit cell are combined in the

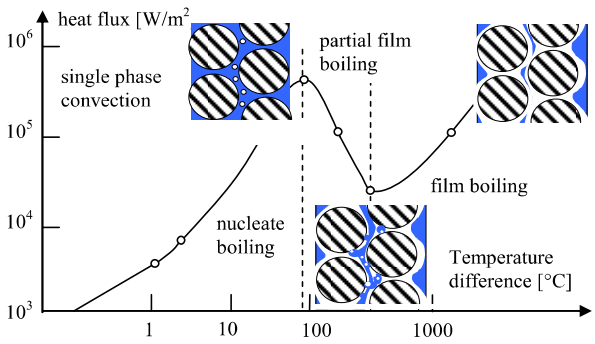

Fig. 6 Flow boiling curve.

model. However, the stratified flow assumed in the model is applicable mostly in the case of film condensation (below saturation temperature) or film boiling (above Leidenfrost temperature) only. Consequently, an improvement of the model is proposed for the nucleate boiling and transition boiling regimes (Fig. 6), where the heat flux depends on bubble nucleation, which is not taken into account in the existing model. The extension of the model which is proposed comes from the theory of flow boiling in small hydraulic diameter channels. Recent studies [23] concluded that neither the nucleate boiling nor turbulent convection are the controlling mechanisms in minichannels. The important process seems to be a transient thin film evaporation where the minichannel flows are typically laminar [24]. Under such conditions, our model describes this thin film evaporation but it is proposed to enhance it by introducing a term of nucleate boiling as follows:

$$h = (1-\alpha)h_{nb} + \left((1-\alpha)h_{cv,l} + \alpha h_{cv,g}\right) \qquad (7)$$

where h is the heat transfer coefficient applied in expression for a specific thermal exchange (Eqs. (4)-(6)). Using the above mentioned equation, the nucleate boiling will be strongly reduced with an increase of vapor quality, which inhibits bubble growth and leads to dry-out at high vapor qualities.

Secondly, heat transfers in the transition zone were also modified. From the PRELUDE measurements of particle temperature, the transition boiling heat fluxes may be estimated as a function of particle temperature. One can obtain the heat flux using the formula:

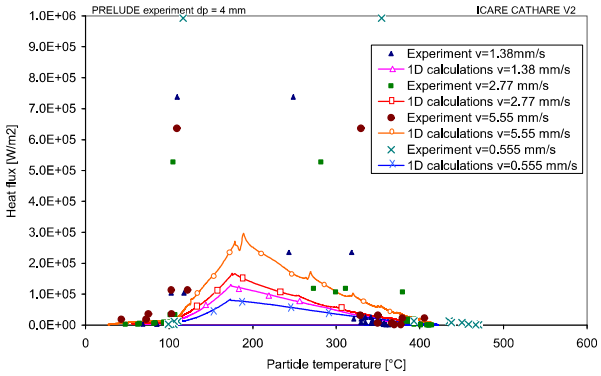

Fig. 7 Experimental and calculated transferred heat flux.

$$Q = \frac{mC_p}{S}\frac{dT}{dt} - \frac{Q_s}{S} \quad (8)$$

where m is the weight of the particle where the thermocouple is located, S is its surface, and Q_s is the maintained volumetric power during reflood. Therefore, the profile and intensity of heat transfer may be reconstructed along the transition boiling range as shown in Fig. 7. From the experimental results, it is observed that the maximum heat flux reached values in the range of 500-1,000 kW/m^2. Compared to experimental results, the calculated heat flux reached lower values. On the other hand, the calculated heat flux reaches yet important values (> 10^5 W/m^2). It is important to note that the experimental heat fluxes presented in Fig. 7 are measured locally where the calculated heat fluxes are averaged for whole mesh volume and as expected, reach lower values. Secondly, from the experimental results, it is not possible to determine the temperature where the maximum heat flux (CHF (critical heat flux)) is achieved because it occurs over a very narrow temperature range (about 10 K). Currently, there is still a lack of information about the critical heat flux in porous media during reflood. Our model, in the absence of specific determination for porous media, uses the Groenveld critical heat flux correlation [25] that depends also on the hydraulic diameter. In order to describe the increasing heat transfer with decreasing surface temperature, a simple cubic dependence on surface temperature was prescribed. The form of the dependence on the surface temperature (parameter ξ) was the matter of a sensitivity study. Currently, the heat flux dependence on void fraction is expressed as:

$$Q = (1-\alpha)(1-\xi)Q_{CHF} + \xi(1-\alpha)Q_{cv,g}$$
$$\xi = \left(\frac{Tw - Tbo}{Tmfs - Tbo}\right)^2 \quad (9)$$

4. Implementation in ICARE-CATHARE

ICARE-CATHARE [9] is a computer code developed by IRSN, designed to describe accurately light water reactor accidental sequences up to a possible vessel failure. It involves advanced models (two-phase multi-dimensional thermal-hydraulics and degradation models) and is built from the coupling of the thermal-hydraulics code CATHARE to the severe accident code ICARE. The above-presented two-phase flow model is implemented in this code. The constitutive heat transfer relations are described in terms of a unique boiling curve from which the code selects the appropriate heat transfer coefficients for both phases (vapor/liquid). For instance, the minimum film stable temperature was set to 400 °C and, mostly, the transition zone and nucleate boiling regime were validated with experimental results.

The ICARE-CATHARE 1D reflood calculations were performed for PRELUDE tests with initial debris bed temperature at 400 °C. The steel particles are placed above a bed of quartz particles, installed in the PRELUDE facility in order to avoid placing a metallic grid which would heat-up because of induction. The homogeneously distributed mass power was set to 210, 170 or 70 W/kg depending on particle diameter. The calculations were performed at atmospheric pressure and for different bottom liquid flow injections (0.555, 1.38, 2.77 and 5.55 mm/s). The temperature of injected water was 20 °C. The objective of the calculations was to validate the model in the prediction of heat fluxes, progression of quench front and steam formation, but also to determine the extent and structure of the two-phase region, for which no information can be deduced from the measurements. In Fig. 7, it is observed that, from the experimental results, the maximum heat flux reached values in the range of 500-1,000 kW/m^2. Compared to experimental results, the calculated heat flux reached lower values. However, the calculated heat flux is sufficiently high (>10^5 W/m^2) to allow rapid quenching thus the quench front velocity and steam production are well predicted.

In Fig. 8 (left), it can be seen that the calculated quench front progression is in good agreement with experimental results for the whole range of liquid injection velocities and particle diameters. Limited discrepancies are observed for the lowest velocity (0.555 mm/s) and 1 mm particles. However, in this test,

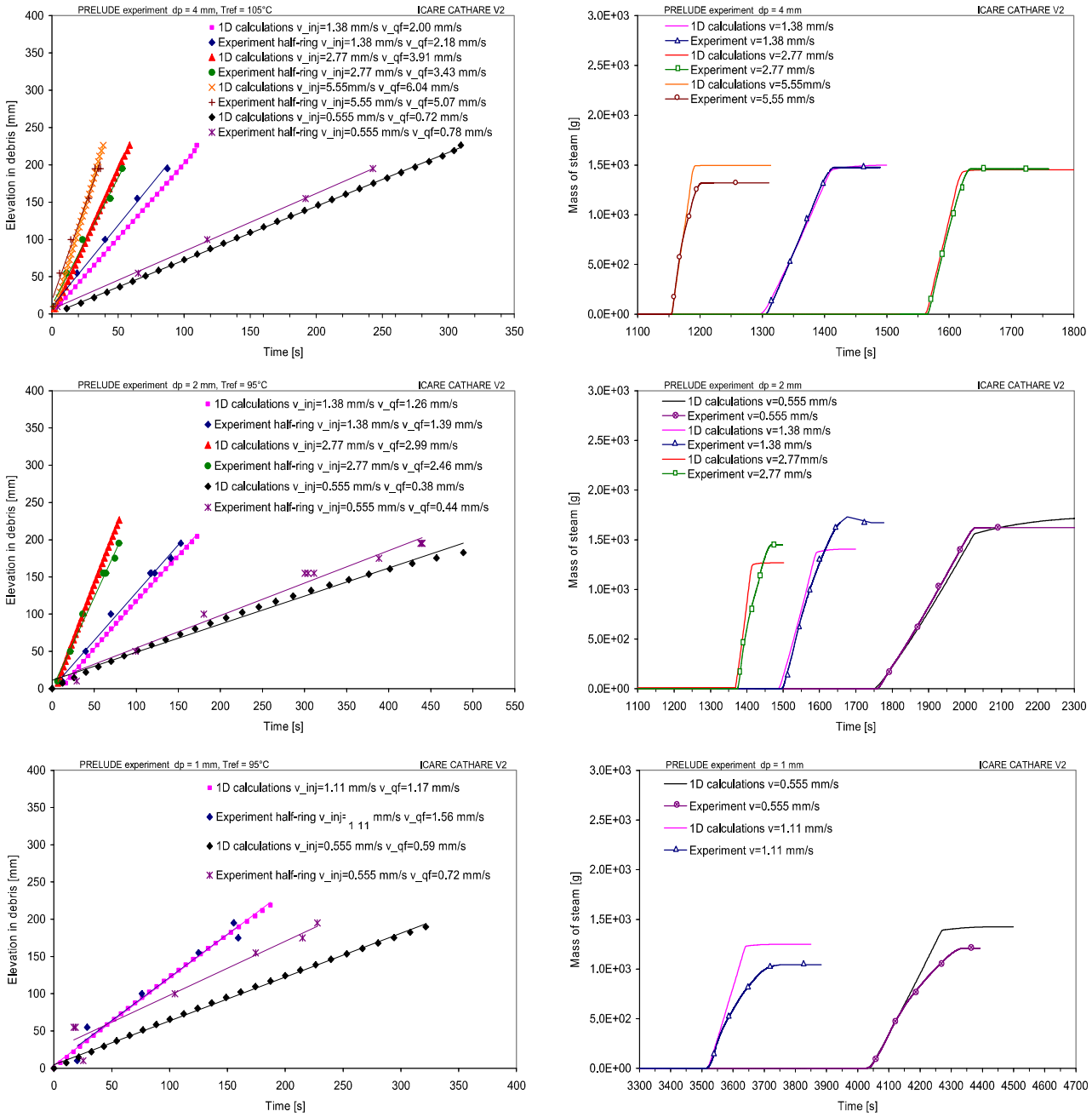

Fig. 8 Quench front velocity (left) and cumulated mass of steam (right).

the quench front velocity at border was higher compared to other rings so the 2D calculations of this test are ongoing. In Fig. 8 (right), the cumulated mass of steam for different tests is plotted as a function of time. From the curve slopes, it can be seen that the time interval in which steam is produced decreases when the injection velocity of liquid increases. This affects the pressure peak which reaches higher values for higher liquid flows (not shown here). On the other hand, the total amount of produced steam is lower. However, at higher injection velocities, water bypassed through the lateral region. When it reached the top of the bed, the steam was partly condensed and the measurements could be influenced. From the calculation results, it can be seen that the slope of the curve for each test corresponds well to experimental results. The

differences in the final steam production are attributed to different initial conditions (temperature is not perfectly uniform in the experiment).

5. Conclusions

The first series of PRELUDE tests has confirmed some of the previous experimental results. Moreover, the results brought new data that contribute to understanding of quenching of a particle bed with bottom cooling injection. The presented analysis concerns the experiments with the debris bed formed with 4 mm, 2 mm or 1 mm particles. The initial temperature was 400 °C. The liquid flow injection at the bottom of test section was 0.555 mm/s, 1.38 mm/s, 2.77 mm/s or 5.55 mm/s. First, the existence of a quasi steady propagation of the quench front is verified for all tests. The quench front velocity depends mainly on the injection velocity and is almost independent of the particle diameter. It is confirmed by both the temperature and pressure measurements. The intensity of heat fluxes was estimated from measurements. This helped to improve the modelling of heat transfers in the transition boiling regime. Comparisons of temperature evolutions at different elevations show that the model is able to predict quenching velocity for different inlet flow rates and different particle diameters, in the whole range covered by PRELUDE experiments. The steam production is also in agreement with experimental results. Calculations clearly show the propagation of a two-phase quench front separating the superheated steam region and the subcooled water region. After a transient evolution resulting in a peak of the quench front velocity, the evolution is steady.

Acknowledgments

The SARNET 2 project of the 7th European framework program is gratefully acknowledged for the transfer knowledge assessment and financial support of debris bed reflooding studies.

References

[1] C. Müller, Review of debris bed cooling in the TMI-2 accident, Nuclear Engineering and Design 236 (2006) 1965-1975.

[2] I. Lindholm, S. Holmströmb, J. Miettinena, V. Lestinenc, J. Hyvärinend, P. Pankakoskib, et al., Dryout heat flux experiments with deep heterogeneous particle bed, Nuclear Engineering and Desighn 236 (19-20) (2006) 2060-2074.

[3] K. Atkhen, SILFIDE experiment: Coolability in a volumetrically heated debris bed, Nuclear Engineering and Design 236 (2006) 2126-2134.

[4] I.V. Kazachkov, Steam flow through the volumetrically heated particle bed, International Journal of Thermal Sciences 41 (2002) 1077-1087.

[5] P. Schäfer, Basic investigations on debris cooling, Nuclear Engineering and Design 236 (2006) 2104-2116.

[6] T. Ginsberg, J. Klein, J. Klages, Y. Sanborn, C.E. Schwarz, J.C. Chen, et al., An Experimental and Analytical Investigation of Quenching of Superheated Debris Beds under Top Reflood Conditions, Report NUREG/CR-4493, 1986.

[7] N.K. Tutu, T. Ginsberg, Debris Bed Quenching under Bottom Flood Conditions, Report NUREG/CR-3850, Sandia National Labs, 1984.

[8] M. Bürger, Validation and application of the WABE code, Nuclear Engineering and Design 236 (2006) 2164-2188.

[9] V. Guillard, ICARE-CATHARE coupling: Three dimensional thermal-hydraulics of severe LWR accidents, in: Proceedings of ICONE-9, Nice, France, 2001.

[10] G. Repetto, Experimental program on debris reflooding (PEARL)—Results on PRELUDE facility, in: Proceedings of NURETH14, Toronto, Canada, Sept. 25-29, 2011.

[11] V.X. Tung, V.K. Dhir, Quenching of a hot particulate bed by bottom quenching, in: Proceedings of ASME-JSME Thermal Engineering Joint Conference, Honolulu, Hawaï, 1983.

[12] F. Duval, F. Fichot, M. Quintard, A local thermal non-equilibrium model for two-phase flows with phase change in porous media, International Journal of Heat and Mass Transfer 47 (3) (2004) 613-639.

[13] N. Trégourès, F. Fichot, F. Duval, M. Quintard, Multi-dimensional numerical study of core debris bed reflooding under severe accident conditions, in: Proceeding of 10th International Topical Meeting on Nuclear Reactor Thermal Hydraulics, Seoul, Korea, 2003.

[14] F. Fichot, O. Marchand, P. Drai, P. Chatelard, M. Zabi´ego, Multi-dimensional approaches in severe accident modelling and analyses, Nuclear Engineering and Design 38 (8) (2006) 733-752.

[15] R.H. Brooks, A.T. Corey, Properties of porous media affecting fluid flow, Journal of the Irrigation and Drainage Division 92 (1996) 61-90.

[16] T. Schulenberg, U. Müller, An improved model for two-phase flow through beds of coarse particles, Int. J. Multiphase Flow 13 (1) (1987) 87-97.

[17] P.C. Carman, The determination of the specific surface area of powder, I. J. Soc. Chem. Ind. 57 (1937) 225-234.

[18] S. Ergun, Fluid flow through packed columns, Chem. Eng. Prog. 48 (1952) 89-97.

[19] F. Duval, Modélisation du renoyage d'un lit de particules: contribution à l'estimation des propriétés de transport macroscopiques (Modeling of reflood of debris bed: contribution to estimation of macroscopic transport properties), Ph.D. Thesis, INPT, Toulouse, France, 2002.

[20] M. Quintard, M. Kaviany, S. Whitaker, Two-medium treatment of heat transfer in porous media: Numerical results for effective properties, Advances in Water Resources 20 (2-3) (1997) 77-97.

[21] F. Petit, F. Fichotb, M. Quintard, Two phase flow in porous medium : Model at local non-equilibrium. (Ecoulement diphasique en milieu poreux: Modèle à non-equilibre local), Int. J. Therm. Sci. 38 (1999) 239-249.

[22] V.X. Tung, V.K. Dhir, A hydrodynamic model for two-phase flow through porous media, Int. J. Multiphase Flow 14 (1988) 47-65.

[23] J.R. Thome, Boiling in microchannels: A review of experiment and theory, Int. J. of Heat and Fluid Flow 25 (2004) 128-139.

[24] A. Mukherjee, Contribution of thin-film evaporation during flow boiling inside microchannels, Int. J. of Thermal Sciences 48 (2009) 2025-2035.

[25] M. Bazin, M. Pellissier, Description of the Base Revision 6.1 Physical Laws Used in the 1D, 0D and 3D Modules, Technical report SSTH/LDAS/EM/2005-038, 2006.